Nanoscale Thin Film Ordering Produced by Channel Formation in the Inclusion Complex of α-Cyclodextrin with a Polyurethane Composed of Polyethylene Oxide and Hexamethylene

ARTICLE *in* MACROMOLECULES · FEBRUARY 2008

Impact Factor: 5.8 · DOI: 10.1021/ma071484n

3 AUTHORS, INCLUDING:

Terence Cosgrove
University of Bristol
245 PUBLICATIONS **5,438** CITATIONS
SEE PROFILE

Andrew N Round
University of East Anglia
31 PUBLICATIONS **527** CITATIONS
SEE PROFILE

Nanoscale Thin Film Ordering Produced by Channel Formation in the Inclusion Complex of α-Cyclodextrin with a Polyurethane Composed of Polyethylene Oxide and Hexamethylene

Erol A. Hasan,[†] Terence Cosgrove,[†] and Andrew N. Round*[,‡,§]

School of Chemistry, University of Bristol, Cantock's Close, Bristol BS8 1TS, UK, and H.H. Wills Physics Laboratory, University of Bristol, Tyndall Avenue, Bristol BS8 1TL, UK

Received July 4, 2007; Revised Manuscript Received December 18, 2007

ABSTRACT: A polyurethane consisting of six blocks of polyethylene glycol and five blocks of hexamethylene diisocyanate was synthesized. The influence of the addition of α-cyclodextrin (α-CyD) on the lower critical solution temperature behavior of the polyurethane was investigated by "cloud point" measurements, and the dependence of the phase state (solution, suspension, and gel) of α-CyD/polyurethane mixtures on the concentration of the two components was determined. The results suggest that the polyurethane forms inclusion complexes with α-CyD and that close to the maximum number of α-CyDs was included. The associative constant of the α-CyD/polyurethane inclusion complex was determined by ^{1}H NMR shift titration using a modified Benesi−Hildebrand equation, and the complex was characterized in the solid state by ^{13}C cross polarization/magic angle spinning NMR and X-ray diffraction. These studies showed that the complexes adopted a channel-like structure. Finally, the morphology of α-CyD/polyurethane complexes in the solid state was visualized by scanning electron microscopy and atomic force microscopy (AFM). AFM images of the inclusion complexes spun-cast on to silicon reveal the existence of ordered domains with heights commensurate with the existence of tetra- and higher-order α-CyD channels. The height quanta of these well-ordered, discrete plateaus point to the dominating influence of the size of the polyethylene glycol blocks within the polyurethane and suggest a route to the production of controlled subnanometer structured surfaces.

Introduction

In recent years, supramolecular chemistry has made great progress. Its aim is to develop highly complex chemical systems from components interacting though intermolecular noncovalent interactions.[1] In this respect, the design of self-assembling systems consisting of cyclodextrin (CyD) and guest molecules has attracted a lot of attention.[2]

CyDs are cyclic oligosaccharides comprising 6, 7, and 8 glucose units (α, *β*, and *γ*) joined by α-1,4-glycosidic linkages. The geometry of CyDs is a truncated cone with a hydrophobic cavity and a hydrophilic exterior.[3] Their hollow structure enables them to host a variety of molecules in the interior.[3,4] In 1990, Harada et al. reported complex formation by the inclusion of polyethylene oxide (PEO) into α-CyD.[5] The complex is produced by penetration of the polymer chain into the empty cavity of the CyD. These types of supramolecular structures are known as polypseudorotaxanes.[6] Since Harada's report, the formation of inclusion complexes between CyDs and different linear homopolymers with polyether,[7−9] polyester,[10−14] polyelectrolyte backbone,[15,16] and some macromolecules with branched architecture[17] has been established.

A recurring subject of investigation remains the mechanism by which inclusion complexes form and the extent to which complete or controlled inclusion, of all monomers of a homopolymer or of all of a particular type of monomer within a copolymer, can be achieved. The degree of inclusion depends strongly on the molecular weight of the included polymer,[5a] while thermodynamic considerations include hydrophobicity and the strength of van der Waals interactions between the polymer and the cavity of the CyD, which in turn tends to correlate with the degree to which the included polymer fills the CyD.[18] Selective threading of CyDs onto part of the polymer chain can be achieved with block copolymers where one of the blocks preferentially forms a complex with CyD, and this behavior has been exploited to reveal details of the mechanism and driving forces behind inclusion.[19−24] This effort has led to the development of complexes with useful functionalities; temperature-responsive polypseudorotaxanes have been synthesized from α-CyD or *β*-CyD and PEO−PPO−PEO that can function as a

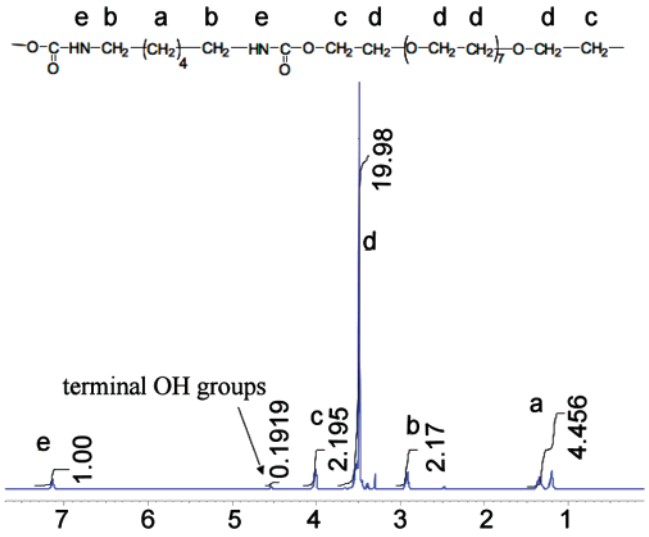

Figure 1. Structure (top) and 1H-NMR spectrum (bottom) of polyurethane composed of PEO 400 and hexamethylene segments. Labeled peaks in the spectrum refer to specific protons as identified in the structure above.

* Corresponding author. E-mail: a.round@uea.ac.uk.
† School of Chemistry, University of Bristol.
‡ H.H. Wills Physics Laboratory, University of Bristol.
§ Current address: School of Chemical Sciences and Pharmacy, University of East Anglia, Earlham Road, Norwich NR4 7TJ, UK.

10.1021/ma071484n CCC: $40.75
Published on Web 01/31/2008

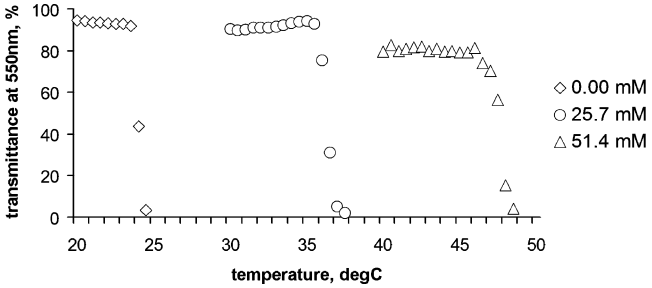

Figure 2. Temperature profiles of clouding of 16 mM polyurethane aqueous solution in the presence of varying amounts of α-CyD.

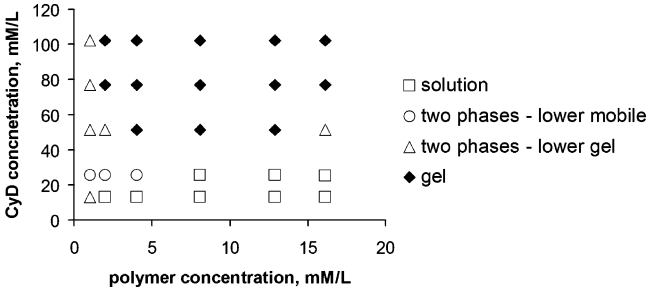

Figure 3. Phase diagram of the inclusion complex between polyurethane and α-CyD.

molecular piston[19] or can be used as a controlled release matrix in protein delivery.[20] Another interesting example is the inclusion complex between biodegradable amphiphilic copolymers and CyDs, which is a novel way to enhance polymer degradability.[21] Studies have been conducted on the behavior of complexes between CyDs and multiblock copolymers consisting of hydrophilic and hydrophobic segments[22,23] in order to establish if threading occurs selectively on the hydrophobic components.

These studies include a report on synthesizing CyD inclusion complexes with polyurethanes.[24] Polyurethanes are multisegmented block copolymers formed from two reagents: a diisocyanate (OCN−R−NCO) and a polyol [HO−(R′−O)$_n$−R′−OH]. They can be readily tailored to produce materials consisting of alternating soft/hard[25,26] or hydrophilic/hydrophobic[27,28] segments. Because of their superior physical and mechanical properties, the polyurethanes are used as biomaterials in many applications such as contact lenses,[29] catheters, and drug delivery systems.[30,31] However, they are known to induce thrombogenic reactions when in contact with blood.[32,33] An interesting approach to avoid this problem could be the penetration of the polyurethane chain into the cavity of the CyD.

In this paper, we have synthesized a water soluble associative polyurethane which consists of polyethylene oxide (hydrophilic) blocks and hexamethylene (hydrophobic) blocks. We have utilized a rational design approach, in which we have taken care to specify block copolymer components and a target molecular weight that favor the maximum extent of inclusion with α-CyD, by choosing components that will give a close fit into the hydrophobic cavity of the cyclodextrin[18] and by targeting a molecular weight low enough to avoid the onset of kinetic effects which limit the extent of inclusion.[5a] Inclusion complex phenomena between α-CyD and the polyurethane were established and investigated by phase studies, NMR, and solid-state characterization techniques. To further characterize the structures formed by the complexation of CyD with the polyurethane synthesized here, we have imaged spun-cast thin films of the polymer and its inclusion complex by atomic force microscopy (AFM). Previously AFM has been used to image individual rotaxane complexes[34] as well as thin spun-cast films of polyrotaxanes.[35]

Experimental Section

Materials. Poly(ethylene glycol) (PEG, Aldrich) with molecular weight (MW) 400 g mol^{-1} was dried under vacuum at 100 °C. 1,6-diisocyanatohexane (HMDI, Acros Organics), triethylamine (Acros Organics), α-CyD (Wacker), and all solvents were used as received.

Synthesis of Polyurethane. Polyurethane was synthesized by the step-growth polymerization of PEG and HMDI using a mole ratio of 6:5 (PEG /HMDI) to target a number average molecular weight (M_n) of ∼3100. The following synthetic procedure was used. A 100 mL, two-neck round-bottom flask was equipped with a magnetic stirrer, nitrogen inlet, and thermocontroller.

PEG (55 mmol) and HMDI (46 mmol) were mixed. Then 0.5 mmol of triethylamine was added as a catalyst to the homogenized mixture. The polymerization process was performed for 16h at 35 °C. The reaction mixture became viscous at the end of the process. Unreacted species and low molecular weight fractions were removed from the product by extraction with toluene.

Polyurethane Characterization. Polyurethane was characterized by ^{1}H NMR and gel permeation chromatography (GPC).

^{1}H NMR. The spectra were taken on a JEOL GX 400 MHz using DMSO as solvent. The composition of the polyurethane was estimated from the relative intensities of methylene protons (3.44 ppm) of the ethylene oxide units and methylene protons (1.21 and 1.35 ppm) of the hexamethylene units. The number average molecular weight of the polymer was estimated from relative intensities of OH groups (4.57 ppm) of PEG blocks and relative intensities of the above spectral lines.

GPC. Size exclusion chromatography (SEC) system type (Viscotek) with a triple detector capability in THF solvent was used for polymer molecular weight determination; the triple detector SEC3 system includes a four-capillary differential viscometer, a right-angle laser light scattering detector (RALLS), and a differential refractometer. Calibration was done with polystyrene standards.

Characterization of α- CyD/Polyurethane Inclusion Complex. *Phase Diagram*. Aqueous stock solutions of α-CyD (12%) or polyurethane (25%) were prepared and left for one night at 5 °C. They were then used to prepare mixtures with different ratios of α-CyD/polyurethane and concentrations at room temperature. The phase transitions that occurred in samples were established visually, by inverting the glass vessels in which they were contained.

^{1}H NMR Titration. Stock solutions of α-CyD (2.5%) or polyurethane (2.5%) were prepared in D_2O and left for one night at 5 °C. Then, they were used to prepare mixtures with different ratios of α-CyD/polyurethane; the concentration of α-CyD was constant (1.25%).

Characterization in the Solid State. To obtain solid materials, the aqueous mixtures of α-CyD/polyurethane were dried under vacuum at room temperature. Solid-state ^{13}C cross polarization/magic angle spinning (CP/MAS) NMR spectra were obtained at 15 kHz on a Bruker DSX 300 MHz NMR spectrometer operating at 303 K. Micrographs were obtained using a JEOL model JSM-5600 scanning electron microscope. The X-ray diffraction measurements were performed with a powder diffractometer (Bruker D8 Advanced: Cu Kα radiation, λ=1.542 Å).

Atomic Force Microscopy. Atomic force microscopy (AFM) was performed on samples prepared from aqueous solutions of α-CyD, polyurethane, and their mixtures, which were deposited onto silicon wafers. The deposition of the samples was performed in two different ways. In the first approach, a drop of a solution was placed onto a silicon wafer and it was left to dry at room temperature. In the second approach, a drop of the solution was placed and spin coated onto the silicon wafer at 3000 rpm over 7 s. Images were obtained in the intermittent contact mode in air with a Multimode Nanoscope IIIa (Veeco) using Olympus cantilevers with a nominal spring constant of 38 N m^{-1}.

Table 1. Phase Diagram of the Inclusion Complex between Polyurethane and α-CyD

	[polymer], mM					
[CyD], mM	1.0	2.0	4.0	8.1	12.9	16.1
12.9	two phases, lower is immobile (PU/CD[a] = 12.9)	solution (PU/CD = 6.4)	solution (PU/CD = 3.2)	solution (PU/CD = 1.6)	solution (PU/CD = 1.0)	solution (PU/CD = 0.8)
25.7	two phases, lower is mobile (PU/CD = 25.7)	two phases, lower is mobile (PU/CD = 12.7)	two phases, lower is mobile (PU/CD = 6.4)	solution (PU/CD = 3.2)	solution (PU/CD = 2.0)	solution (PU/CD = 1.6)
51.4	two phases, lower is immobile (PU/CD = 51.4)	two phases, lower is immobile (PU/CD = 25.5)	gel (PU/CD = 12.7)	gel (PU/CD = 6.4)	gel (PU/CD = 4.0)	two phases, lower is immobile (PU/CD = 3.2)
77.0	two phases, lower is immobile (PU/CD = 77.0)	gel (PU/CD = 38.2)	gel (PU/CD = 19.1)	gel (PU/CD = 9.6)	gel (PU/CD = 6.0)	gel (PU/CD = 4.8)
102.3	two phases, lower is immobile (PU/CD = 102.3)	gel (PU/CD = 51.0)	gel (PU/CD = 25.5)	gel (PU/CD = 12.7)	gel (PU/CD = 8.0)	gel (PU/CD = 6.4)

[a] PU/CD = mol ratio of polyurethane to α-CyD.

Results and Discussion

The structure of the polyurethane synthesized is shown in Figure 1. The copolymer is composed of hydrophilic (polyethylene glycol) and hydrophobic (hexamethylene) segments. The 1H-NMR (Figure 1) and GPC (data not shown) data confirm that the polyurethane has a molecular weight of 3100; the ratio of intensities of the major methylene protons in the PEO (3.44 ppm) to the terminal hydroxyl protons (4.57 ppm) was 19.98:0.1919, or 99.9:1, compared to the expected 96:1 for the structure with a molecular weight of 3100, and the ratio of hexamethylene protons (1.21 and 1.35 ppm) to hydroxyl protons was 4.456:0.1919, or 22.28:1, compared to the expected 20:1. Such structures can be compared to hydrophobe-modified ethoxylated urethane (HEUR) polymers, which are well known for their associative properties[27,28,36] and lower critical solution temperature (LCST)[36] behavior in water. HEUR polymers are block copolymer polyurethanes consisting of PEO and alkyl segments; they are generally far larger than the polyurethane we have synthesized and exhibit their desired properties only when terminated by alkyl segments, again in contrast to our material which is terminated by PEO segments. The aqueous solutions of the copolymer in this study clouded when heated to above room temperature.

The cloud point of the polyurethane aqueous solution shifts to higher temperatures with increasing α-CyD concentration (Figure 2). A similar influence of CyDs on water solutions of an elastin-like thermoresponsive polypentapeptide has been reported by Alonso et al.[37] The effect of the CyDs on the thermal response has been attributed to the formation of an inclusion complex between the CyD rings and the apolar parts of the polymer chain upon which intra- and interchain hydrophobic interactions are hindered, shifting the clouding effect to a higher temperature.[37−39] Binding constants of CyD inclusion complexes decrease. Some of these complexes even start to decompose with increasing temperature,[40−44] promoting the reappearance of hydrophobic interactions between the polymer chains. Thus, the clouding of the polymer/CyD aqueous system occurs at higher temperatures.

Phase Diagram. In many papers, it has been reported that after threading of CyD onto the polymer chain the system can undergo a transition to a two-phase system or gel.[5−17] This behavior has been explained by the formation of hydrogen bonds between adjacent CyD molecules on the same polymer chain and critically between CyD molecules on neighboring polymer chains, which act as physical cross-links causing network formation.

In Table 1 and Figure 3, the phase states of different mixtures of the polyurethane and the α-CyD are shown. The α-CyD/polyurethane inclusion complex appeared in three different states depending on the concentration and the ratio of components: solution, two-phase separation with the lower phase being mobile or immobile, and gel. The phase diagram clearly shows the concentration range of each phase state. At lower concentrations of α-CyD (12.9 and 25.7 mM), the inclusion complex appears as a solution at lower α-CyD/polyurethane ratios, presumably because the concentration of threaded CyD rings on the polymer chains is not enough for aggregation. But in the same concentration range of α-CyD, the inclusion complex undergoes a two-phase separation at the higher α-CyD/polyurethane ratios. Apparently, there is a critical concentration of threaded CyD rings for their interchain aggregation into microcrystals and hence phase separation. Therefore, in the higher concentration range of α-CyD (51.4−102.3 mM), the inclusion complex appears as a two-phase separation or gel but not as a solution.[17]

To make better sense of the phase diagram, the dependence of changes in the phase state of the inclusion complex on polymer concentration will be discussed. In the lowest polymer concentration (1 mM), each of the α-CyD/polyurethane mixtures undergoes phase separation (Figure 4a). On increasing the polymer concentration (2 mM), the α-CyD/polyurethane inclusion complex appears in two states: solution at the lowest α-CyD/polyurethane ratio and gel at higher ratios. The phase separated state is observed at intermediate ratios (Figure 4b). The appearance of the solution state is explained, as in the case discussed above, by the low concentration of threaded α-CyD rings, whereas the gel formation can be explained by the well-known overlapping behavior of macromolecules at higher polymer concentrations. The overlapping effect favors the interchain aggregation of threaded CyD rings into microcrystals, which act as "cross-links" to organize the threaded polymer chains in a network structure throughout the system.[23] The inclusion complex appears phase separated at intermediate α-CyD/polyurethane ratios, presumably because the concentration of threaded α-CyD rings on the polymer chains is below that is needed to form enough cross-links for network formation. With further increase of the polymer concentration, the phase separated state disappears in the phase diagram (8.1 and 12.9 mM of polymer). This may be attributed to the dominating overlapping of macromolecules, which favors interchain aggregates of CyD rings. But the phase separation state again appears at the highest polymer concentration (16.1 mM),

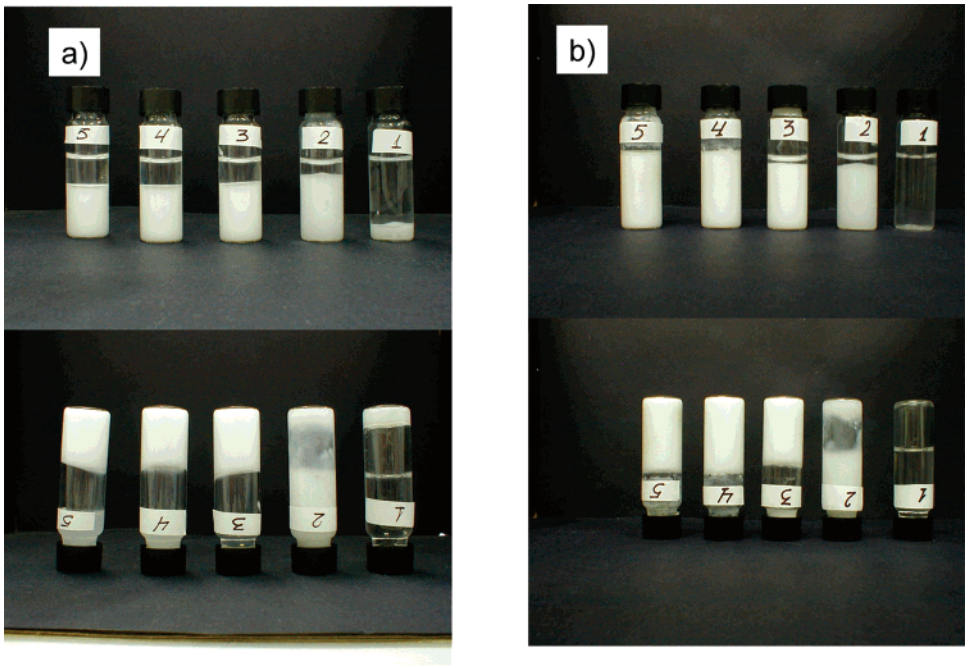

Figure 4. Photographs of aqueous mixtures contain (1) 1.285, (2) 2.75, (3) 5.139, (4) 7.709, and (5) 10.279 mM of α-CyD and (a) 0.101 or (b) 0.202 mM of polyurethane.

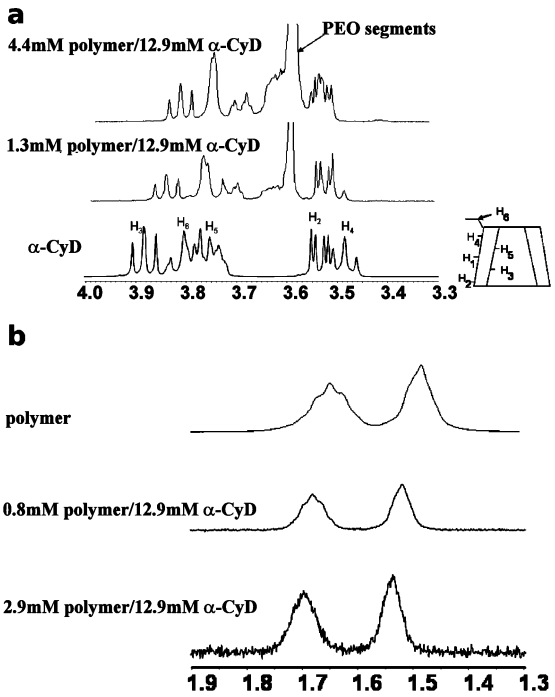

Figure 5. ^{1}H NMR spectra of α-CyD and α-CyD/polyurethane mixtures in D_2O: (a) the region characteristic of the protons of cyclodextrin; (b) the region characteristic of the hexamethylene protons.

presumably because the concentration of strung α-CyD rings is too low to be compensated with the overlapping effect of polymer chains.

To gain more of an insight into the formation of the inclusion complex between the α-CyD and the polyurethane, the supernatants of the phase-separated samples at the lowest polymer concentration were investigated by ^{1}H NMR. The supernatants of the mixtures with the lower ratios (12.7 and 25.4) contained both α-CyD and polyurethane, whereas the supernatants of the mixtures with higher α-CyD/polyurethane ratios (51.0, 76.5, and 102.0) only contained α-CyD. From these results, information can be extracted about the stoichiometry of the inclusion complex between α-CyD and polyurethane. It is well known that the stoichiometry of ethylene oxide monomer units/α-CyD is 2:1,[7] whereas the binding model of hexamethylene units/α-CyD has a stoichiometry of 1:1.[43] Hence, the number of α-CyD rings needed for full inclusion of the polyurethane under this investigation is 32. The estimated value is between the mixture with a CyD/polyurethane ratio of 25.4, in which the supernatant contained both α-CyD and polyurethane, and the mixture with a CyD/polyurethane ratio of 51.0, where the supernatant contained only the α-CyD. This suggests that nearly the whole polymer chain is threaded by α-CyD rings at the higher CyD/polyurethane ratio, in contrast to the report of Olson et al.[23] of inclusion complex formation between α-cyclodextrin and block copolymers of similar composition but much larger molecular weight (between 19 and 44 kg/mol), where the stoichiometries observed were much lower than would be expected for complete occupancy. This difference may be attributed to the insolubility in water of the unthreaded polymers in the study by Olson et al. (in contrast to the solubility demonstrated by our material in Figure 2) and is consistent with the effect observed by Harada et al.[5a] that the degree of polymerization of a given polymer exerts a strong kinetic effect on the degree of inclusion complexation.

^{1}H NMR Shift Titration. NMR shift titration is one of the most frequently used methods to determine associative constants of guest compounds with host CyDs.[44−48] To apply this method, we investigated aqueous α-CyD/polyurethane mixtures with different ratios of the components by ^{1}H NMR. Our results showed a continuous change in chemical shifts of inner α-CyD protons (H3 and H5) with increasing α-CyD concentration (Figure 5a). A similar mode of chemical shift changes was also established for the protons of the hexamethylene segments of the polymer (Figure 5b**)**. But it was impossible to investigate any chemical shift changes for the peak corresponding to PEO segments in ^{1}H NMR spectra because it was broad and nonuniform.[23]

The established chemical shift changes in ^{1}H NMR spectra of α-CyD/polyurethane mixtures clearly indicate the inclusion of polymer chain in the CyD cavity and demonstrate that the

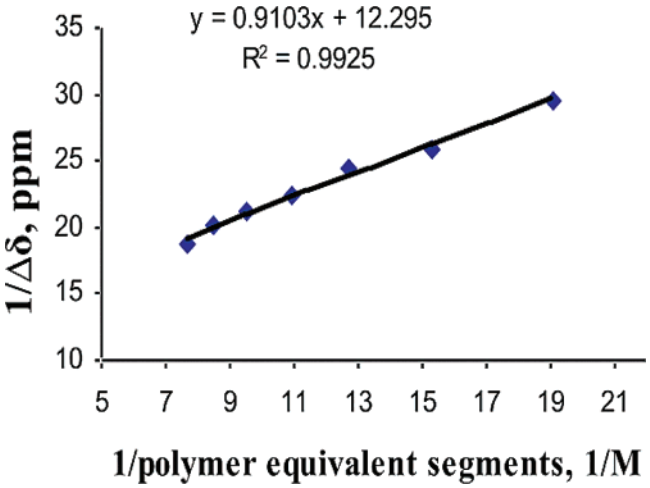

Figure 6. A Double reciprocal plot of chemical shift changes, $\Delta\delta$, of H3 of α-CyD vs concentration of polymer equivalent "segments" of polyurethane.

system is in a fast exchange regime between free and complex species.[49,51] Therefore, the observed signal is a population average of their chemical shifts. The equilibrium constant (K_c) of α-CyD/polyurethane complex was estimated by the modified Benesi−Hildebrand equation.[50−52]

$$1/\Delta\delta = 1/(K_c\Delta\delta_{max}[G]_o) + 1/\Delta\delta_{max} \quad (1)$$

where $\Delta\delta = (\delta_{host} - \delta_{obs})$, $\Delta\delta_{max} = (\delta_{host} - \delta_{HG})$, G = guest, and H = host. The modified Hildebrand−Benesi equation is only useful for systems with a 1:1 inclusion complex between host and guest, which can be represented by:

$$[H] + [G] \rightleftharpoons [HG] \text{ and } K_c = [HG]/[H][G] \quad (2)$$

Another limitation of the Hildebrand-Benesi method is that it is only valid when one is observing species H in the presence of a large excess of species G. To adjust our system to Hildebrand−Benesi conditions, the following assumptions were made. The polymer chain was divided into 32 equiv "segments", which correspond to the number of CyD rings needed to cover the whole polymer chain. Consequently, the inclusion complex can be expected at a ratio of 1:1 between the α-CyD and the equivalent segment, and the concentration of guest segments is in excess of the concentration of host CyDs.[16] Thus, we overcome both the above mentioned limitations.

In Figure 6, the double reciprocal plot shows a linear dependence between the chemical shift changes of the inner H3 proton of α-CyD and polymer concentration. The equilibrium constant (K_c) of α-CyD/polymer equivalent segment was calculated from the slope of the fitting curve using the above mentioned modified Hildebrand−Benesi equation. The estimated K_c was 12.35 M^{-1} (the linear fit equation is shown on the plot). As already mentioned, the investigated polyurethane is composed of PEG and hexamethylene blocks that can both form of inclusion complexes with α-CyD. The published values of K_c are about 700 M^{-1} for 1-hexanol[43] and 65 M^{-1} for α,ω-diaminohexanes,[53] highlighting the importance of the end group in pseudorotaxane formation, whereas K_c for hydrophilic PEG[54] is about 20 M^{-1}. As mentioned above, the threaded CyD rings are in a dynamic state, which means they are not settled on one part of the polymer chain but are able to move along it. Because the PEO part in the polyurethane is dominant (78 wt % of polyurethane is PEO), the probability of CyD rings being on the PEO blocks is higher. Therefore the estimated K_c value of the polyurethane (12.35 M^{-1}) can be expected to be near to the K_c of the homopolymer of PEG (about 20 M^{-1}).

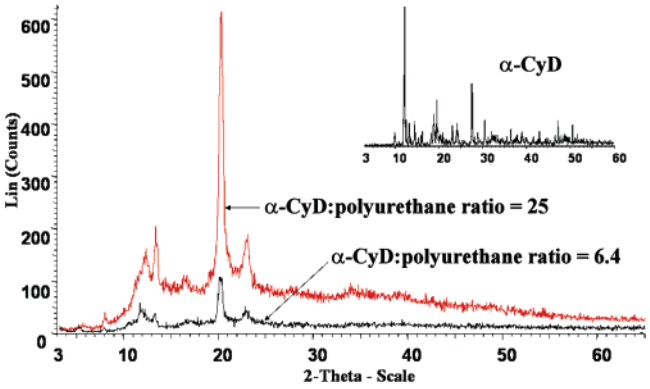

Figure 7. X-ray powder diffractograms of α-CyD and dried gels of α-CyD/polyurethane complex.

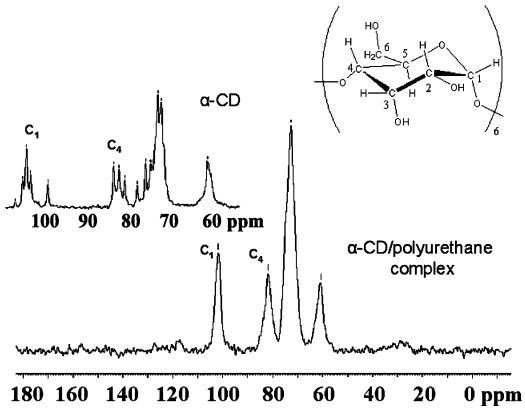

Figure 8. ^{13}C CP/MAS NMR spectra of α-CyD and dried supramolecular gel α-CyD/poly urethane complex.

Inclusion Complex of α-CyD and Polyurethane in Solid State. To gain insight into the structure of the inclusion complex of α-CyD/polyurethane, dried samples were investigated by X-ray diffraction, solid NMR, and SEM.

Figure 7 gives the X-ray diffraction patterns of the α-CyD/polyurethane complex for two different ratios of the two components and the pattern of pure α-CyD. As one can see, the diffraction patterns of the inclusion complex are very different to pure α-CyD. It is well known that the peak at $2\theta \approx 20°$ in the diffraction pattern of α-CyD/polyurethane complex is characteristic of the channel structure of α-CyD when including long guest molecules and polymers, in particular.[7,55] The results also clearly show the increasing intensity of the characteristic peak of inclusion complexes with α-CyD owing to increasing of the crystal channel structure.

Conformational changes of α-CyD rings when they include a polyurethane chain were investigated by solid-state NMR. Figure 8 shows ^{13}C CP/MAS NMR spectra of the free α-CyD and inclusion α-CyD/polyurethane complex. The α-CyD is known to assume a less symmetrical conformation in the crystalline uncomplexed state.

In this case, the spectrum shows resolved C-1 and C-4 resonances. Especially, resonances for C-1 and C-4 adjacent to a single conformational strained glycosidic linkage are observed in the spectrum. In contrast, the resolved resonances disappear in the spectra of the inclusion complex and each carbon of the glucose unit is observed as a single peak.[56] The results indicate that the α-CyD rings in the inclusion complex state adopt a symmetrical conformation and each glucose unit is in a similar environment.

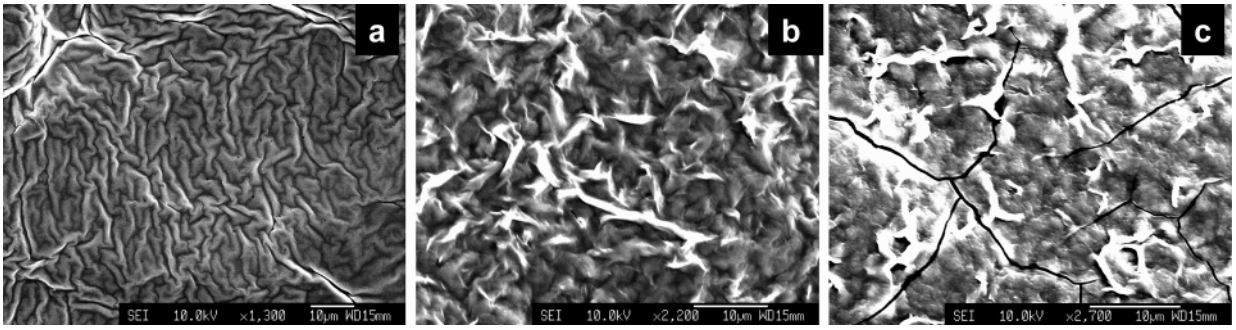

Figure 9. SEM micrographs of the polyurethane film (a) and the dried supramolecular gels produced from aqueous solutions containing 2 mM of polyurethane and 51 mM of α-CyD (b) or 77 mM of α-CyD (c).

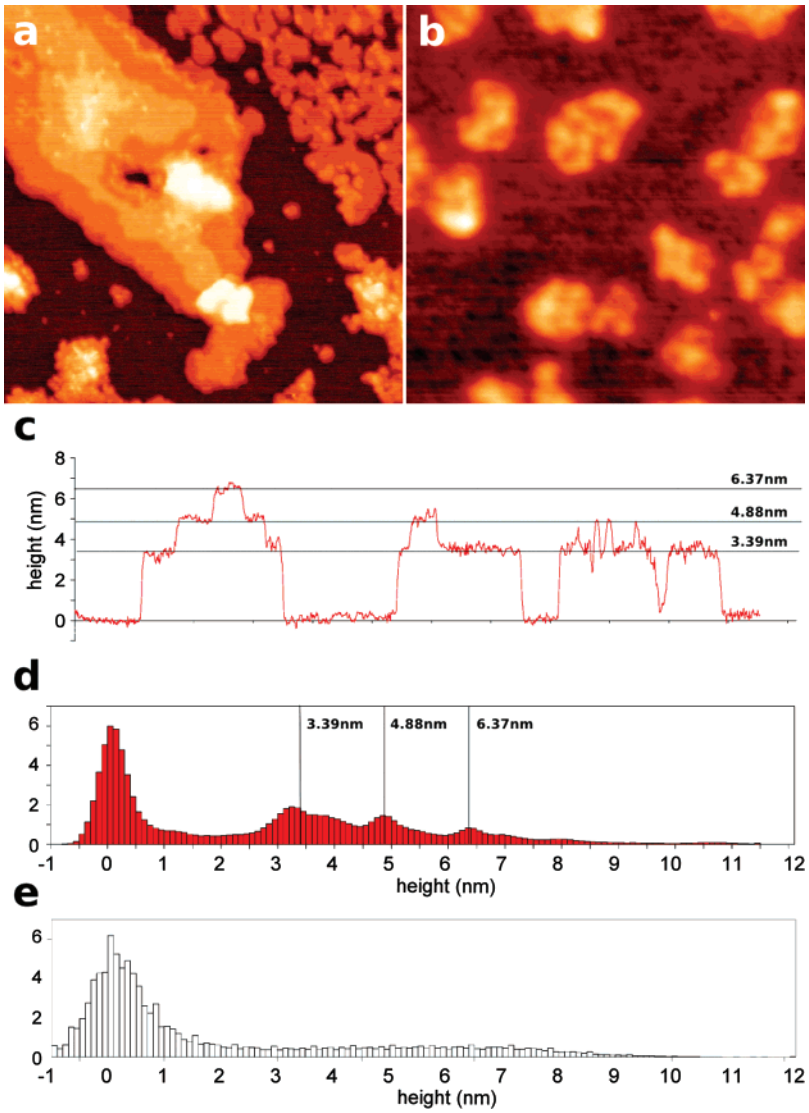

Figure 10. (a) AFM image of α-CyD and polyurethane complex spun cast on to silicon: image size = 2300 × 2300 nm, *z*-scale = 12 nm. (b) AFM image of polyurethane obtained under the same conditions as above: image size = 2300 × 2300 nm, z-scale = 12 nm. (c) Line trace taken from Figure 10a showing the heights of the predominant plateaus together with the peak values of Gaussian curves fitted to peaks in the histogram of heights in Figure 10a. (d) and (e) histograms of the heights in panels a and b of Figure 10, respectively; *y*-axis are percentages.

The morphology of the inclusion complex of α-CyD/polyurethane was visualized by SEM microscopy. Figure 9 shows SEM images of dried samples obtained from an aqueous solution of polyurethane and from aqueous mixtures of its inclusion complex with α-CyD in three different ratios of the components. The polyurethane film shows a "cerebral-like" morphology. At the lower α-CyD/polyurethane ratio, parts of the polyurethane chain are included in the α-CyD rings, which act as physical cross-links between polymer chains. As a result, the observed morphology is more complicated and "wrinklier" than the former one. But with increasing the α-CyD/polyurethane ratio, the inclusion complex transforms to a smooth morphology, owing to the full inclusion of the polymer chain in α-CyD rings.

Atomic force microscopy was used to investigate thin films of the polyurethane and its inclusion complex at various ratios

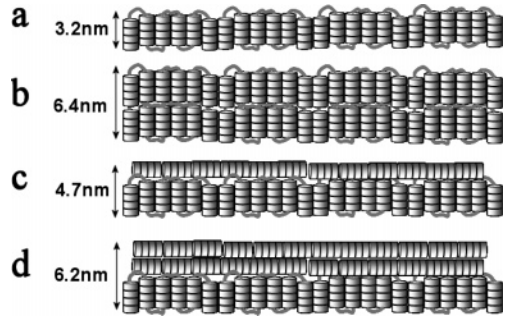

Figure 11. Proposed structures of the polyurethane/α-CyD inclusion complexes accounting for the first (a), second (c), and third (b,d) peaks in the height histogram and line trace in Figure 10. Cylinders represent α-CyD, and threads represent polymer segments.

of α-CyD/polyurethane. AFM is a very powerful method for investigating the nanoscale structure of materials deposited onto a surface. The accuracy of AFM imaging is dependent on certain parameters of the investigated material such as thickness, roughness, etc. These parameters are critically dependent on the method of sample deposition. Therefore, in one case, the samples were deposited on the surface by simple evaporation of water and imaging was carried out by amplitude-modulated dynamic force microscopy in air. In this case, images of the resultant films of both the inclusion complex and the polyurethane alone resembled those observed below in Figure 10b. On the other hand, the spin-coating method, which is a well-known method for preparation of uniform nanoscale films, produced very different results. Figure 10a depicts a typical view of the surface structure adopted by the α-CyD/polyurethane inclusion complexes upon deposition. A striking feature of this image is the presence of several well-defined plateaus with uniform heights and discrete boundaries, which are absent from images of the polyurethane sample prepared in the same way (Figure 10b). Topographical heterogeneity is observed in the images of the polyurethane on silicon, which may reflect ordering in the polymer structure on the basis of hydrophobicity, but the structures formed are ill defined and no peaks in the height histogram are seen.

A line profile (Figure 10c) through some typical examples of the plateaus shows their heights above the substrate together with the results of fitting multiple Gaussian peaks to a histogram of the heights in a representative image. Panels d and e of Figure 10 show, respectively, histograms of the heights in the images of the inclusion complex formed by α-CyD and the polyurethane and the polyurethane alone. Peaks corresponding to the heights observed in the line trace are prominent features of the inclusion complex histogram but are absent in the polymer histogram.

The peak values observed for the plateau heights (3.39 ± 0.22, 4.88 ± 0.14, 6.37 ± 0.25, 8.06 ± 0.46, and 10.13 ± 0.99 nm) are very close to the values expected of integer multiples of the ring depths of α-CyD (0.8 nm), corresponding to 4, 6, 8, 10, and 13 α-CyDs, respectively, suggesting that the structure created by formation of the inclusion complexes is derived from the order induced by channel formation by the included α-CyDs. The PEO moieties of this polymer can accommodate four α-CyDs which would, if stacked perpendicularly to the surface with the hexamethylene segments acting as flexible hinges, have a height of approximately 3.2 nm, corresponding closely to the height of the first plateau. Such an arrangement implies that when the rotaxane adopts this structure upon spin coating onto the substrate the hexamethylene segments of the copolymer are no longer included (or are only partially included) by cyclodextrin, allowing these segments to act as flexible hinges. Adding a second and third layer of such structures accounts for the third and fifth peaks. Alternatively, allowing one or more of the channel structures to stack horizontally on the first layer accounts for all subsequent peaks, given the 1.5 nm diameter of α-CyD. The images do not show plateaus with heights commensurate with a single, horizontal layer on silicon (i.e., at 1.5 nm). Figure 11 depicts the proposed structures. The observation of such structuring and its attribution to the underlying structure of the polyurethane suggest together that this approach offers a route to creating structures with controlled subnanometer scale steps.

Conclusions

In summary, we have synthesized a polyurethane consisting of alternating segments of polyethylene glycol and hexane and showed that it forms spontaneously an inclusion complex with α-cyclodextrin. Consideration of the phase diagram of mixtures of α-CyD and the polyurethane along with ^{1}H NMR of the supernatants in the case of two-phase systems suggests that nearly all available inclusion sites on both the ethylene oxide and hexamethylene components of the block copolymer are occupied, while ^{1}H NMR shift titration provides an estimate of the association constant for the inclusion complex. Characterization of this inclusion complex in the solid state by ^{13}C CP/MAS NMR, X-ray diffraction, and AFM demonstrates that the α-CyDs included in the complex adopt a channel structure. In particular, the AFM data reveals previously unobserved behavior when the polyrotaxane is deposited on to silicon by spin coating, suggesting that the formation of α-CyD channels in the regular structures thus formed is regulated by the lengths of the PEO segments and that the process of spin coating induces a shift from inclusion of the hexamethylene units to inclusion of the PEO segments only. Thereby, a route to the noncovalent synthesis of ordered surface films of well-defined subnanometer scale with many of the properties attributed to block copolymer polypseudorotaxanes is created. Future work will explore the mechanisms governing the self-assembly of these structures and the limits of this approach.

References and Notes

(1) (a) Lehn, J. M. *Supramolecular Chemistry*: *Concepts and Perspectives*; Wiley-VCH: Weinheim, 1995. (b) Lehn, J. M. *Science* **2002**, *295*, 2400−2403. (c) Lehn, J. M. *Proc. Natl. Acad. Sci. U.S.A.* **2002**, *99*, 4763.

(2) (a) Jullien, L.; Canceill, J.; Valeur, B.; Bardez, E.; Lefavre, J.-P.; Lehn, L.-M.; Marchi-Artzner, V.; Pansu, R. *J. Am. Chem. Soc.* **1996**, *118*, 5432−5442. (b) Li, G.; McGown, L. B. *Science* **1994**, *264*, 249−251. (c) Uekama, K.; Hirayama, F.; Irie, T. *Chem. Rev.* **1998**, *98*, 2045−2076.

(3) Bender, M. L.; Komiyama, M. *Cyclodextrin Chemistry*; Springer: Berlin, 1978.

(4) (a) Szejtli, J. *Chem. Rev.* **1998**, *98*, 1743−1753. (b) K. B. Lipkowitz, *Chem. Rev.* **1998**, *98*, 1829−1873.

(5) (a) Harada, A.; Kamachi, M. *Macromolecules* **1990**, *23*, 2821−2823. (b) Harada, A.; Kamachi, M. *J. Chem. Soc., Chem. Commun.* **1990**, 1322−1323.

(6) Gibson, H. W.; Bheda, M. C.; Engen, P. T. *Prog. Polym. Sci.* **1994**, *19*, 843−945.

(7) Harada, A.; Li, J.; Kamachi, M. *Macromolecules* **1993**, *26*, 5698−5703.

(8) Harada, A.; Suzuki, S.; Nakamitsu, T.; Okada, M.; Kamachi, M. *Koubunshi Ronbunshu* **1995**, *52*, 594−598.

(9) Harada, A.; Okada, M.; Li, J.; Kamachi, M. *Macromolecules* **1995**, *28*, 8406−8411.

(10) Harada, A.; Kawaguchi, Y.; Nishiyama, T.; Kamachi, M. *Macromol. Rapid Commun.* **1997**, *18*, 535−539.

(11) Kawaguchi, Y.; Nishiyama, T.; Okada, M.; Kamachi, M.; Harada, A. *Macromolecules* **2000**, *33*, 4472−4477.

(12) Harada, A.; Nishiyama, T.; Kawaguchi, Y.; Okada, M.; Kamachi, M. *Macromolecules* **1997**, *30*, 7115−7118.

(13) Shuai, X.; Porbeni, F. E.; Wei, M.; Bullions, T.; Tonelli, A. E. *Macromolecules* **2002**, *35*, 3778−3780.
(14) Shin, K.; Dong ,T.; He, Y.; Taguchi, Y.; Oishi, A.; Nishida, H.; Inoue, Y.; *Macromol. Biosci.* **2004**, *4*, 1075−1083.
(15) Herrmann, W.; Keller, B.; Wenz, G.; *Macromolecules* **1997**, *30*, 4966−4972.
(16) Meier, L.; Heule, M.; Caseri, W.; Shelden, R.; Suter, U. *Macromolecules* **1996**, *29*, 718−723.
(17) (a) Born, M.; Ritter, H. *Angew. Chem., Int. Ed. Engl.* **1995**, *34*, 309−311. (b) Born, M.; Ritter, H. *Adv. Mater.* **1996**, *8*, 149−151. (c) Topchieva, I. N.; Gerasimov, V. I.; Panova, I. G.; Karezin, K. I.; Efremova, N. V. *Polym. Sci., Ser. A* **1998**, *40*, 171. (d) Jiao, H.; Goh, S. H.; Valiyaveettil, S. *Macromolecules* **2002**, *35*, 1980. (e) Sabadini, E.; Cosgrove, T. *Langmuir* **2003**, *19*, 9680−9683.
(18) Wenz, G.; Han, B.-H.; Muller, A. *Chem. Rev.* **2006**, *106*, 782−817.
(19) Fujita, H.; Ooya, T.; Yui, N. *Macromolecules* **1999**, *32*, 2534−2541.
(20) Li, J.; Li, X.;.Zhou, Zh.; Ni, X.; Leong, K. *Macromolecules* **2001**, *34*, 7236−7237.
(21) Li, J.; Li, X.;.Zhou, Zh; Ni, X.; Leong, K. *Macromolecules* **2003**, *36*, 1209−1214.
(22) Weickenmeier, M.; Wenz, G. *Macromol. Rapid Commun.* **1997**, *18*, 1109−1115.
(23) Olson, K.; Chen, Y.; Baker, G. *J. Polym. Sci., Part A: Polym. Chem.* **2001**, *39*, 2731−2739.
(24) Yamaguchi, I.; Takenaka, Y.; Osakada, K.; Yamamoto, T. *Macromolecules* **1999**, *32*, 2051−2054.
(25) Noshay, A.; McGrath, J. E. *Block Copolymers: Overview and Critical Survey*; Academic Press: New York, 1977.
(26) Oertel, G. *Polyurethane Handbook*, 2nd ed.; Hanser: New York, 1993.
(27) May, R.; Kaczmarski, J.; Glass J.; *Macromolecules* **1996**, *29*, 4745−4753.
(28) Kaczmarski, J.; Glass, J. *Langmuir* **1994**, *10*, 3035−3042.
(29) Haschke, E.; Sendijarevic, V.; Wong, S.; Frisch, K. C.; Hill, G. *J. Elastomers Plast.* **1994**, *26*, 41−57.
(30) McNeill, M. E.; Graham, N. B. *J. Biomater. Sci., Polym. Ed.* **1993**, *4*, 305−322.
(31) Bae, Y. H.; Kim, S. W. *Adv. Drug Delivery Rev.* **1993**, *11*, 109−135.
(32) Abraham, G. A.; Roman, J. S. *Biomaterials* **2002**, *23*, 1625−1638.
(33) Lee, J. H.; Ju, Y. M.; Kim, D. M. *Biomaterials* **2000**, *21*, 683 −691.
(34) van den Boogaard, M.; Bonnet, G.; van't Hof, P.; Wang, Y.; Brochon, C.; van Hutten, P.; Lapp, A.; Hadziioannou, G. *Chem. Mater.* **2004**, *16*, 4383−4385.
(35) Cacialli, F.; Wilson, J.; Michels, J.; Daniel, C.; Silva, C.; Friend, R.; Severin, N.; Samori, P.; Rabe, J.; O'Connell, M.; Taylor, P.; Anderson, H. *Nat. Mater.* **2002**, *1*, 160−164.
(36) Alami, E.; Abrahmsen-Alami, S.; Vasilescu, M.; Almgren, M. *J. Colloid Interface Sci.* **1997**, *193*, 152−162.
(37) Alonso, M.; Arranz, D.; Reboto, V.; Rodríguez-Cabello, J. C. *Macromol. Chem. Phys.* **2001**, *202*, 3027−3034.
(38) Han, J. S.; Yoo, M. K.; Sung, Y. K.; Lee, M. Y.; Cho, S. C. *Macromol. Rapid Commun.* **1998**, *19*, 403−407.
(39) Cooper, A. I.; McAuley-Hecht, E. K. *Philos. Trans. R. Soc. London, Ser. A* **1993**, *345*, 23.
(40) Rekharsky, M. V.; Schwarz, F. P.; Tewari, Y. B.; Goldberg, R. N. *J. Phys. Chem.* **1994**, *98*, 4098−4103.
(41) Ikeda, T.; Lee, K. W.; Ooya, T.; Yui N.; *J. Phys. Chem. B* **2003**, *107*, 14−19.
(42) Martin Del Valle, E. M. *Process Biochem.* **2004**, *391*, 1033−1046.
(43) Bastos, M.; Briggner, E. L.; Shehatta, I.; Wadsö, I. *J. Chem. Thermodyn.* **1990**, *22*, 1181−1190.
(44) Kanda, Y.; Yamamoto, Y.; Inoue, Y.; Chûjô, R.; Kobayashi, S. *Bull. Chem. Soc. Jpn.* **1989**, *62*, 2002−2008.
(45) Lehmann, J.; Kleinpeter, E.; Krechl, J. *J. Inclusion Phenom.* **1991**, *10*, 233−239.
(46) Salvatierra, D.; Diez, C.; Jaime, C. *J. Inclusion Phenom.* **1997**, *27*, 215−231.
(47) Butkus, E.; Jose, J. C.; Berg, U. *J. Inclusion Phenom.* **1996**, *26*, 209−218.
(48) Schneider, H.; Hacket, F.; Rudiger, V. *Chem. Rev.* **1998**, *98*, 1755−1785.
(49) Hwang, J. H.; Lee, S.; Park, W. J. *Bull. Korean Chem. Soc.* **2000**, *21*, 245−250.
(50) Fielding, L. *Tetrahedron* **2000**, *56*, 6151−6170.
(51) Hanna, M. W.; Ashbaugh, A. L. *J. Phys. Chem.* **1964**, *68*, 811−816.
(52) Mathur, R.; Becker, E. D.; Bradley, R. B.; Li, N. C. *J. Phys. Chem.* **1963**, *67*, 2190−2194.
(53) Avram, L.; Cohen, Y. *J. Org. Chem.* **2002**, *67*, 2639−2644.
(54) Horsky, J. *Eur. Polym. J.* **1998**, *34*, 591−596.
(55) Rusa, C. C.; Bullions, A. T.; Fox, J.; Porbeni, E. F.; Wang, X.; Tonelli, E. A. *Langmuir* **2002**, *18*, 10016−10023.
(56) Harada, A. *Adv. Polym. Sci.* **1997**, *133*, 141−201.

MA071484N